Ultrathin Two-Dimensional MnO2/Graphene Hybrid Nanostructures for High-Performance, Flexible Planar Supercapacitors

ARTICLE *in* NANO LETTERS · APRIL 2013

Impact Factor: 13.59 · DOI: 10.1021/nl400600x · Source: PubMed

6 AUTHORS, INCLUDING:

Lele Peng
University of Texas at Austin
25 PUBLICATIONS **869** CITATIONS

NANO LETTERS

Letter

pubs.acs.org/NanoLett

Ultrathin Two-Dimensional MnO_2/Graphene Hybrid Nanostructures for High-Performance, Flexible Planar Supercapacitors

Lele Peng,[†,‡] Xu Peng,[§] Borui Liu,[‡] Changzheng Wu,*[,†] Yi Xie,*[,†] and Guihua Yu*[,‡]

[†]Hefei National Laboratory for Physical Sciences at the Microscale, University of Science and Technology of China, Hefei, Anhui, 230026, P. R. China

[‡]Materials Science and Engineering Program and Department of Mechanical Engineering, The University of Texas at Austin, Austin, Texas 78712, United States

[§]School of Materials Science and Engineering, Wuhan Institute of Technology, Wuhan, Hubei, 430073, P. R. China

Supporting Information

ABSTRACT: Planar supercapacitors have recently attracted much attention owing to their unique and advantageous design for 2D nanomaterials based energy storage devices. However, improving the electrochemical performance of planar supercapacitors still remains a great challenge. Here we report for the first time a novel, high-performance in-plane supercapacitor based on hybrid nanostructures of quasi-2D ultrathin MnO_2/graphene nanosheets. Specifically, the planar structures based on the δ-MnO_2 nanosheets integrated on graphene sheets not only introduce more electrochemically active surfaces for absorption/desorption of electrolyte ions, but also bring additional interfaces at the hybridized interlayer areas to facilitate charge transport during charging/discharging processes. The unique structural design for planar supercapacitors enables great performance enhancements compared to graphene-only devices, exhibiting high specific capacitances of 267 F/g at current density of 0.2 A/g and 208 F/g at 10 A/g and excellent rate capability and cycling stability with capacitance retention of 92% after 7000 charge/discharge cycles. Moreover, the high planar malleability of planar supercapacitors makes possible superior flexibility and robust cyclability, yielding capacitance retention over 90% after 1000 times of folding/unfolding. Ultrathin 2D nanomaterials represent a promising material platform to realize highly flexible planar energy storage devices as the power back-ups for stretchable/flexible electronic devices.

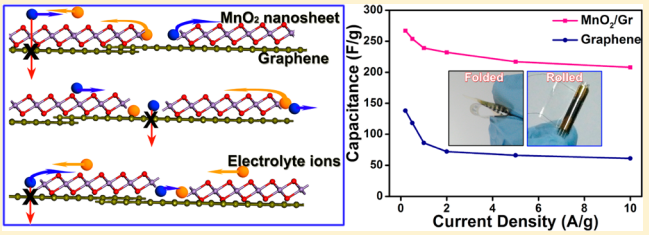

KEYWORDS: *Planar supercapacitor, birnessite δ-MnO_2, ultrathin nanosheets, all-solid-state, layer-by-layer assembly, energy storage*

The development of compliant all-solid-state power back-ups with high energy and power densities is critical to the emerging flexible electronics technology.[1] Recently, all-solid-state in-plane supercapacitors have been developed to promise a rich combination of planar energy devices that could be alternative candidates of power supplies for stretchable/flexible electronics.[2] Planar supercapacitors with two-dimensional extensions and confined space in the vertical direction possess versatile capabilities to be folded, rolled up, or even reshaped into other architectures, exhibiting very promising flexibility without adverse effect on the device performance. Therefore, the 2D in-plane designs for supercapacitors show great potential as highly integrated energy devices and systems for many stretchable/flexible electronic devices such as smart sensors and actuators, stretchable displays, and flexible touch screens.[3−8]

Planar supercapacitors, as a new emerging branch of electrochemical capacitors (ECs), could enable the entire device to be much thinner and flexible.[9−11] In such device, the electrolyte ions are transported two-dimensionally and thus shorten the ion travel distance by eliminating the necessity of a separator. Planar supercapacitors significantly decrease the thickness in the vertical direction and rather expand along the 2D horizontal planes, making compact device design possible. However, there are still very few material platforms that have been exploited to realize the high-performance planar supercapacitors. The past few decades have witnessed substantial progress on the development of high-capacitive-performance transition metal oxides (TMOs), such as RuO_2, MnO_2, Co_3O_4, and NiO,[12−17] but their non-2D structures greatly hinder them from being effectively integrated to the in-place device configuration of planar supercapacitors. 2D graphene and quasi-2D graphene-like materials are the promising prototype materials for planar supercapacitors given their atomic layer thickness and the flat morphology. Recently, graphene nanosheets or VS_2 nanosheets were successfully introduced to construct the in-plane supercapacitors with reasonable performance.[18,19] However, the layer-by-layer tight stacking in their thin film form inevitably diminishes the interlayer space between homogeneous ultrathin nanosheets, which could significantly hinder the electrolyte ion diffusion.

Received: February 15, 2013
Revised: March 16, 2013
Published: April 16, 2013

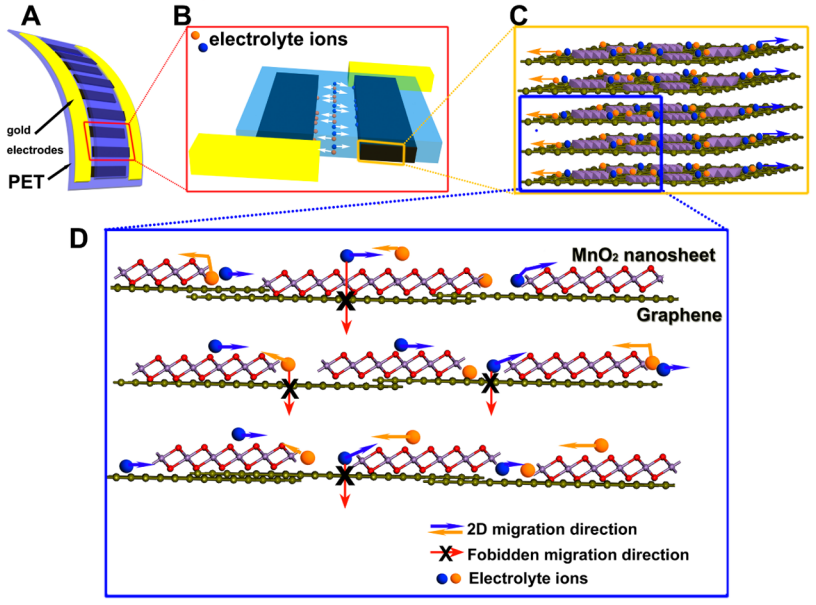

Figure 1. Design of hybrid 2D δ-MnO_2/graphene structures based planar supercapacitors. (A) Schematic illustration of the ultraflexible planar supercapacitor, constructed by the hybrid film as the working electrode, the current collector, and gel electrolyte on plastic polyethylene terephthalate (PET) substrate. (B) The planar supercapacitor unit showing that the 2D hybrid thin film functions as two symmetric working electrodes. (C) The hybrid thin film was stacked by the layers of chemically integrated quasi-2D δ-MnO_2 nanosheets and graphene sheets. (D) Schematic description of the 2D planar ion transport favored within the 2D δ-MnO_2/graphene hybrid structures.

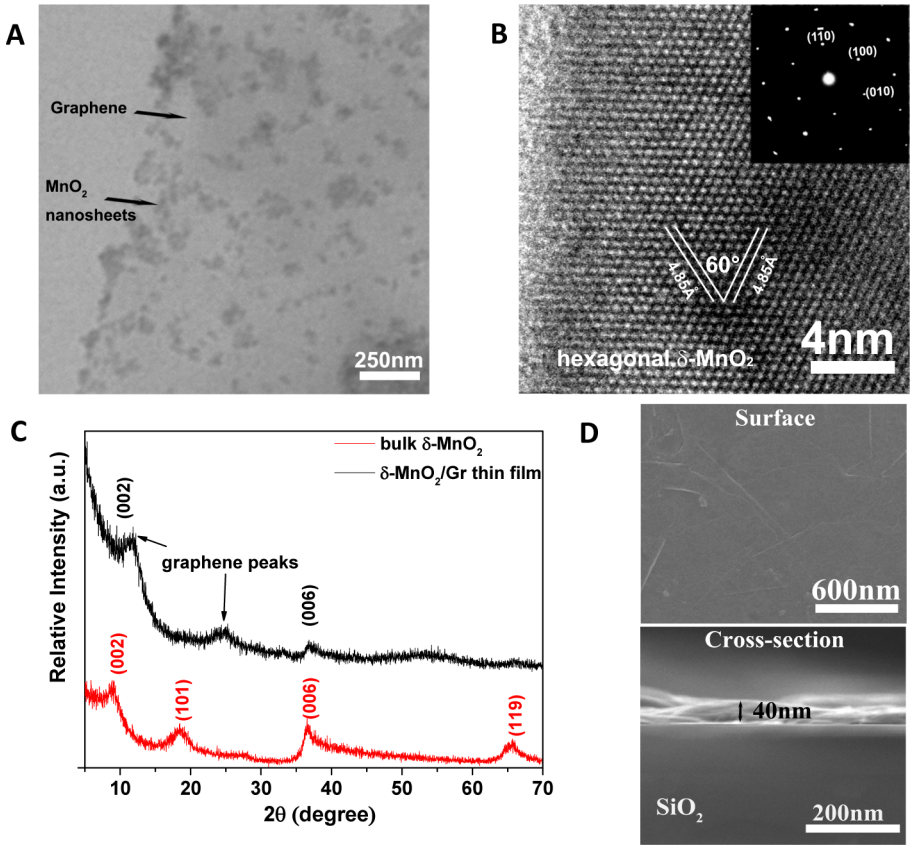

Figure 2. Characterization of planar hybrid structures of δ-MnO_2 nanosheets integrated on graphene. (A) TEM image of the 2D hybrid structure with δ-MnO_2 nanosheets integrated on graphene surfaces. (B) HRTEM image of a typical δ-MnO_2 nanosheet exfoliated from the 2D δ-MnO_2/graphene hybrid structures. Inset: SA-ED pattern of δ-MnO_2 nanosheet showing the hexagonal symmetry. (C) XRD patterns of the bulk δ-MnO_2 (red) and the assembled 2D δ-MnO_2/graphene hybrid film (black). (D) SEM images showing the surface and cross-section of hybrid thin film, indicating the smooth surface with the average film thickness of ~40 nm.

dx.doi.org/10.1021/nl400600x | *Nano Lett.* 2013, 13, 2151−2157

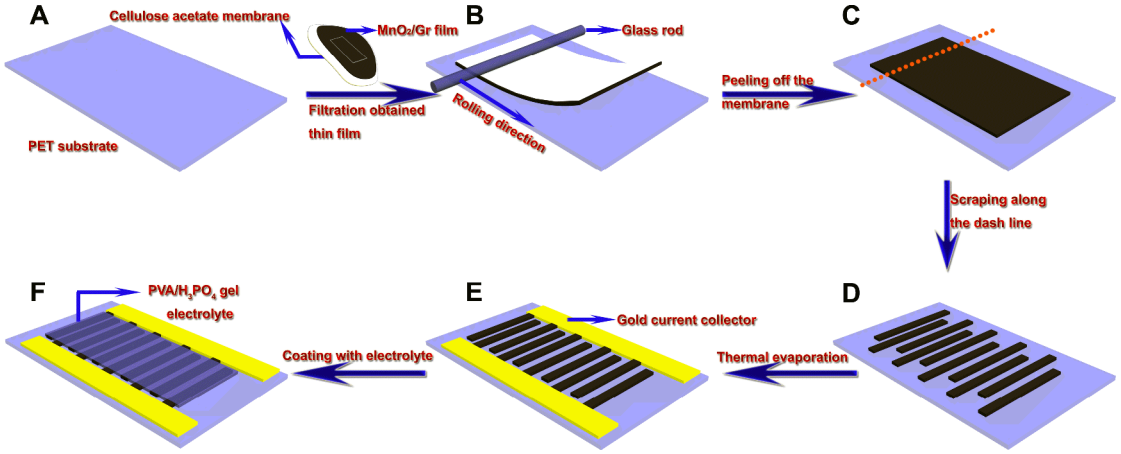

Figure 3. Schematic of fabrication procedures for ultraflexible planar supercapacitors. (A–C) Transferring 2D δ-MnO_2/graphene hybrid thin film onto plastic PET substrates: The 2D hybrid thin film on the surface of cellulose acetate membrane was obtained by a vacuum filtration process, followed by tightly pressing thin film onto PET substrates and peeling off the cellulose acetate membrane, leading to freestanding 2D hybrid thin film on target substrates. (D) Obtaining strips of hybrid thin film by scraping along the dashed line as the working electrodes. (E) Two columns of gold current collectors were thermally evaporated on each side of the working electrodes. (F) The planar supercapacitor was finally established after coating PVA/H_3PO_4 gel electrolyte on the parallel region filling the channel between two working electrodes.

Here we present a novel hybrid nanostructure composed of distinct quasi-2D ultrathin nanosheets for greatly enhanced supercapacitor performance, as shown in Figure 1. Specifically, the planar structures based on the δ-MnO_2 nanosheets integrated on graphene sheets can introduce more electrochemically active surfaces for absorption/desorption of the electrolyte ions and bring extra interface at the hybridized interlayer areas to facilitate charge transport during charging/discharging processes, offering good rate capability and cycling stability. In addition, the integrated δ-MnO_2 nanosheets serving as active centers for the pseudocapacitive reactions contribute to the great enhancement of the specific capacitance. Meanwhile, the δ-MnO_2 integrated on graphene can potentially tailor the distance between each sheet of densely stacked graphene and open up the interlayer space to allow for more electrolyte ions to penetrate efficiently into the hybridized film. Consequently the hybrid 2D nanostructure design enhances the electrochemical performance of as-fabricated planar supercapacitors. Moreover, the pseudocapacitive δ-MnO_2 nanosheet introduces high redox capacitance (theoretically ~1300 F/g for MnO_2) and greatly improves the electrochemical performance even at a relative low mass loading with an ultrathin layer.[20,21]

The planar structure of the designed δ-MnO_2/graphene hybrid is obtained by chemically integrating δ-MnO_2 nanosheets on graphene due to the strong electrostatic interaction in the solution treatment process. The charge behavior has evidenced that the water-exfoliated δ-MnO_2 nanosheet is electronegative and DMF-exfoliated graphene is electropositive (see Supporting Information parts S1–S4). In our case, graphene sheets were synthesized by reducing graphene oxides (GO) with hydrazine, which were prepared from purchased graphite powders with a grain size of 20 μm according to a modified Hummers' method.[22,23] δ-MnO_2 nanosheets were exfoliated from the bulk δ-MnO_2, which was oxidized from Mn^{2+} in a mild oxidative environment.[24] After an intercalation/extraction process of water molecules, the bulk δ-MnO_2 was exfoliated into single layered δ-MnO_2 nanosheets, forming a homogeneous dispersion with a typical Tyndall effect.[25] TEM and AFM images in Figure S5 show the flat morphology of the MnO_2 nanosheets with an ultrathin atomic thickness of ~1.0 nm. Exfoliated graphene sheets shown in TEM and AFM images of Figure S5 exhibit an average size of ~4 μm. The graphene sheets with large area and flat morphology serve as ideal microscopic substrates to host the δ-MnO_2 nanosheets to a maximum areal utilization. The synergic effects of the electrostatic interaction and the flat morphology between the quasi-2D δ-MnO_2 nanosheets and 2D graphene realized the integration of δ-MnO_2 nanosheets onto graphene surfaces. Figure 2A shows the TEM image of the hybrid nanostructure, indicating that δ-MnO_2 nanosheets were well-integrated on graphene sheets. Moreover, HR-TEM image and SAED pattern projected along c axis as shown in Figure 2B, in which the interplanar spacing was measured to be 0.485 nm, further confirm the presence of high-quality δ-MnO_2 integrated on the graphene surfaces.

To make the best of the designed planar structures, it is critical to develop a reliable method to obtain the transferable ultrathin films with controlled thickness and orientation. Meanwhile device fabrication of the oriented thin films relies on the structural design of material scaffolds. 2D graphene and quasi-2D graphene-like materials with the planar extensions provide a promising material platform to fabricate c-oriented thin films. In our case, the hybrid planar structures of δ-MnO_2 integrated on graphene were used to fabricate the 2D hybrid film as the working electrodes via a conventional vacuum filtration process, similar to that previously reported for fabricating flexible graphene films.[26] The vacuum filtration method is adopted in our studies because self-limiting flow fields can produce films with controllable thickness and promote the assembly of hybrid nanostructures of quasi-2D δ-MnO_2/graphene nanosheets in the c-orientation. Thin film X-ray diffraction (XRD) patterns were used to verify the c-orientation of self-assembled 2D δ-MnO_2/graphene hybrid thin films. As shown in Figure 2C, only the peaks of (002) and (006) facets can be detected, indicating a well-defined c-orientation of the 2D δ-MnO_2/graphene hybrid thin film. In Figure 2D, the SEM image of the surfaces of the hybrid thin film revealed the smooth and flat morphology of in-plane structure. The layered structure of the hybrid thin film could be clearly seen in the cross-sectional SEM image, with an average

dx.doi.org/10.1021/nl400600x | Nano Lett. 2013, 13, 2151–2157

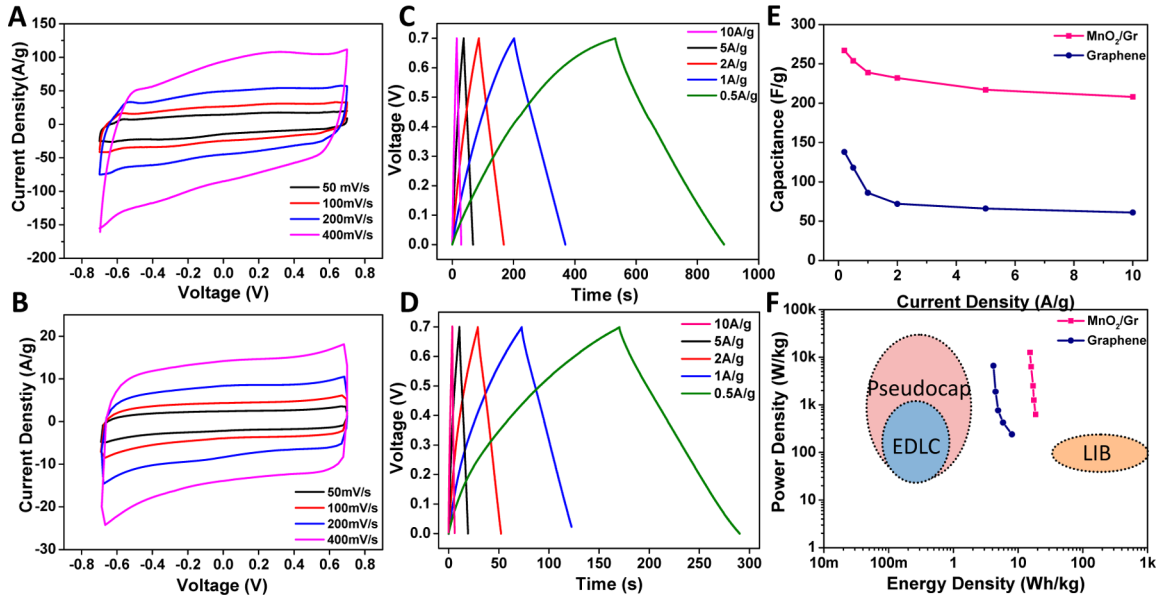

Figure 4. Electrochemical performance of the planar supercapacitors based on 2D δ-MnO_2/graphene hybrid thin film. (A) Rate-dependent CV curves for planar supercapacitors based on the 2D δ-MnO_2/graphene hybrid at different scan rates (from 50 to 400 mV/s). (B) CV curves for planar supercapacitors based on graphene. (C) Galvanostatic charge−discharge curves of the planar supercapacitor based on the hybrid at various current densities (0.5 A/g to 10 A/g). (D) Galvanostatic curves of the supercapacitor based on graphene-only. (E) Comparison of specific capacitance values for the supercapacitors based on hybrids and based on graphene. (F) A typical Ragone plot of as-fabricated supercapacitors.

thickness of ∼40 nm, indicating thin thickness of the hybrid thin film. The microscopic planar structure of hybrid materials provided the 2D transport pathway for the electrolyte ions and was further assembled into a macroscopic film, providing the material platform for planar supercapacitors.

Assembly and transfer of ultrathin 2D nanosheet based materials onto large-area substrates are the essential processes for fabricating planar devices, especially for planar supercapacitors which require the integration of the whole device components into a two-dimensional configuration on the same horizontal plane. Briefly, a rectangle strip of the 2D δ-MnO_2/graphene hybrid thin film obtained by vacuum filtration was rolled with a glass rod onto the flexible PET substrate, followed by tightly pressing and peeling off the cellulose acetate membrane. This procedure led to the transfer of freestanding 2D hybrid thin film on the target substrate, as shown in Figure 3C. Notably, hybrid 2D δ-MnO_2/graphene thin films can be transferred onto a range of substrates such as PET, quartz, glass, and silicon wafer (Figure S5). By scraping along the dashed line as shown in Figure 3C and D, slim strips of the transferred thin film were obtained as the working electrodes for the planar supercapacitor. After repeated scrapings for construction of an array of parallel lines as primary units of the working electrodes, two columns of gold current collectors were thermally evaporated on each side of the working electrodes and integrated the primary units into a typical planar supercapacitor device. The all-solid-state planar supercapacitor was finally established after filling the channel between two working electrodes with gel electrolyte of PVA/H_3PO_4, as demonstrated in Figure 3F.

The planar hybrid nanostructure of quasi-2D δ-MnO_2/graphene nanosheets is a key factor to enhance the electrochemical performance of in-plane supercapacitors. To evaluate the electrochemical performance of the planar supercapacitor based on the 2D δ-MnO_2/graphene hybrid film, we performed cyclic voltammetry (CV), galvanostatic charge−discharge (CD), and electrochemical impedance spectroscopy (EIS) tests using a two-electrode system. The as-fabricated planar supercapacitors based on 2D δ-MnO_2/graphene hybrid structures have brought significant electrochemical performance enhancement, as clearly shown in Figure 4. A set of rate-dependent CV curves of the planar supercapacitor based on 2D δ-MnO_2/graphene hybrid (Figure 4A) and planar supercapacitor based on graphene only (Figure 4B) were acquired at various scan rates from 50 to 400 mV/s within −0.7 to 0.7 V voltage window. The nearly rectangular CV curves at different scan rates indicated the efficient intralayer charge transfer and the nearly ideal capacitive behaviors.[27,28] Note that there are no apparent redox peaks observed at the voltage range of −0.7 to 0.7 V, which reveals that electrode materials based on MnO_2 nanosheets can be stabilized by PVA/H_3PO_4 gel electrolyte. At the same scan rates, Figure 4A and B show that the resulting rectangle areas from CVs of planar supercapacitor based on δ-MnO_2/graphene hybrids are substantially larger than those for planar supercapacitor based on graphene, suggesting that specific capacitance values of hybrid MnO_2/graphene planar supercapacitor are much higher than those for graphene-only based devices. Although high theoretical pseudocapacitance of transition metal oxides can significantly increase the capacitance of supercapacitor devices compared to electric double layer capacitors, in many of previously reported works,[29−31] the high values were obtained at relatively low scan rates (1−10 mV/s), making these supercapacitor devices lose advantages for being primary energy storage devices with high rate capability. In contrast, a high specific capacitance of ∼200 F/g is accomplished in our studies under a high scan rate of 400 mV/s. Moreover, the enhanced electrochemical performance was confirmed by galvanostatic charge−discharge measurements performed under different current densities (from 0.5 to 10 A/g). Figure 4C and D shows that, at the same current density of 1 A/g, the charge−discharge time for δ-MnO_2/graphene hybrid system was substantially prolonged (>100%

dx.doi.org/10.1021/nl400600x | Nano Lett. 2013, 13, 2151−2157

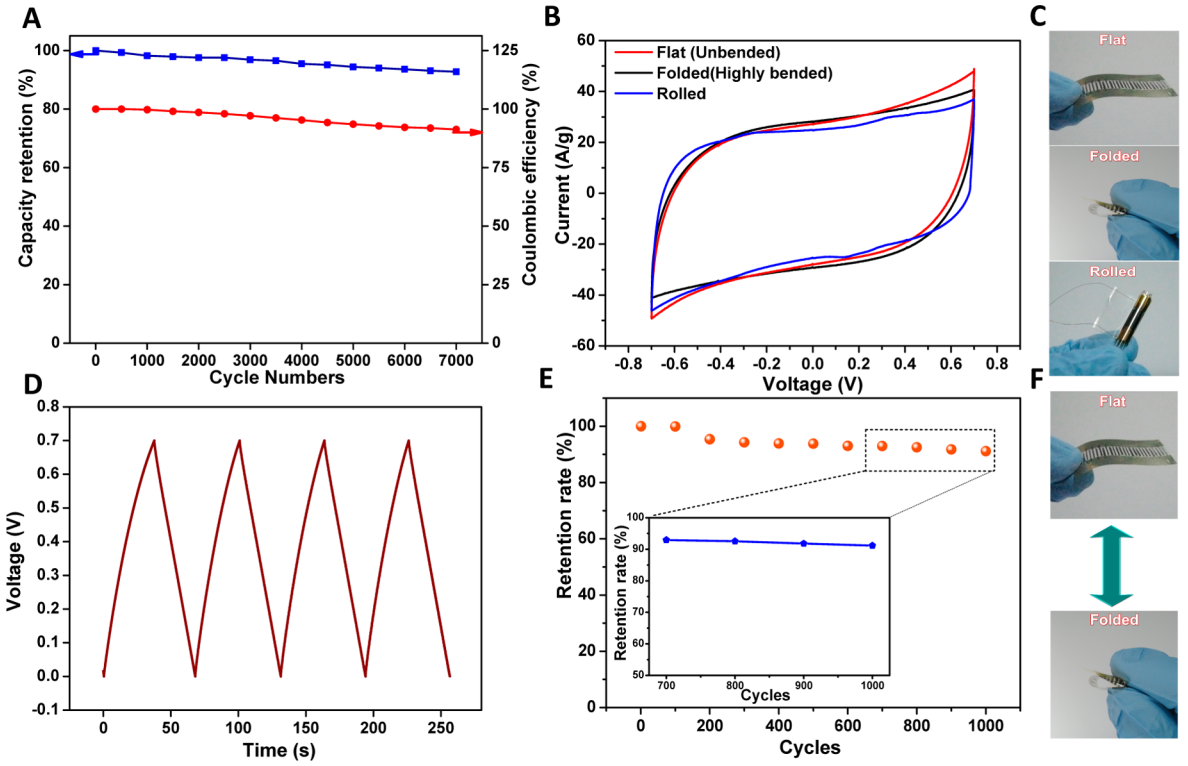

Figure 5. Cycling performance of ultraflexible planar supercapacitors based on hybrid thin film. (A) Capacitance retention (blue) and Coulombic efficiency (red) of the planar supercapactior device over 7000 charge/discharge cycles. (B) CV curves for the planar supercapacitor under three different bending states. (C) Demonstration of three different bending states: flat, folded, and rolled. (D) Typical CD curves of the planar supercapacitor based on hybrid thin film at current density of 5 A/g. (E) Cycling stability under repeated flat/folded cycles. (F) Demonstration of the flat/folded cycle when testing cycling stability.

increase) over graphene system, and the linear voltage−time profile and highly symmetric charge/discharge characteristics were indicative of good capacitive behavior achieved by hybrid electrode systems. The specific capacitance can be derived from the CD curves (see SI, part S8).[32] Accordingly, the as-fabricated in-plane supercapacitor based on the hybrid planar nanostructure yielded specific capacitances of 254, 249, 232, 217, and 208 F/g at current densities of 0.5, 1, 2, 5, and 10 A/g, respectively, as summarized in Figure 4E. Meanwhile, the planar supercapacitor based on δ-MnO_2/graphene hybrid exhibited better rate capability, with only ∼22% capacitance loss when current density increases by a factor of 20 (from 0.5 to 10 A/g) compared to ∼56% loss for graphene-based electrodes. The enhanced capacitance and rate capability can be attributed to rational design of 2D δ-MnO_2/graphene hybrid structures, which synergize the effects of both efficient 2D ion transport possible in the same horizontal plane and additional interfaces and pseudocapactance brought by δ-MnO_2 nanosheets.

To further evaluate the energy efficiency of as-fabricated planar supercapacitors based on the planar hybrid nanostructures of MnO_2/graphene, energy density (E) and power densities (P) were calculated from CD curves (see SI, part S8). Figure 4F shows the Ragone plot of the as-obtained planar supercapacitor based on δ-MnO_2/graphene hybrid and compares specific E and P with those for pseudocapacitors, electrical double-layer capacitors (EDLC), and lithium ion batteries (LIBs). As shown in the Ragone plot, the MnO_2/graphene hybrid based planar supercapacitors deliver a high energy density of 17 Wh/kg at a power density of 2520 W/kg, superior to graphene based planar supercapacitors. Moreover, the maximum energy density of 18.64 Wh/kg and the highest power density of 12.6 kW/kg are achieved for the hybrid δ-MnO_2/graphene based planar supercapacitor, which are comparable to other previously reported carbon nanomaterials/MnO_2 based traditional supercapacitors (see SI,Table 1 for detailed comparison), revealing that as-established planar supercapacitors would be a promising candidate to serve as high-energy power supply components in planar flexible electronics.

Good cycling stability is another critically important characteristic for planar supercapacitors based on hybrid nanostructures of 2D δ-MnO_2/graphene. Owing to the good compressibility and mechanical extensibility possible with the planar ultrathin films, our planar supercapacitors achieved excellent cycling performance with impressive flexibility. CV and CD measurements were performed to illustrate these promising device characteristics. Figure 5A demonstrates that the as-fabricated planar supercapacitors based on 2D δ-MnO_2/graphene hybrid film showed an excellent cycle life. After over 7000 times of charging/discharging cycles, the capacitance retention rates remained over 92%, and the Coulombic efficiency was still kept at ∼91%, indicating remarkable cycling stability of our planar supercapacitors. Taking advantage of PVA/H_3PO_4 gel as the electrolyte,[33] we stabilized the planar structure to realize better capacitance retention and cyclability (see SI part S10). CV curves of the planar supercapacitor under different bending states were measured at the scan rate of 100 mV/s to explore the feasibility to fabricate an ultraflexible planar supercapacitor (Figure 5B). Indeed, there only exist slight differences in specific capacitances of the planar supercapacitor based on δ-MnO_2/graphene hybrid when tested under three bending states. Note that this hybridized thin film

dx.doi.org/10.1021/nl400600x | Nano Lett. 2013, 13, 2151−2157

has no noticeable structural destruction even after being folded or rolled thousands of times, which cannot be realized using conventional three-dimensional building blocks. The demonstrated ultrahigh flexibility for hybrid 2D δ-MnO_2/graphene nanosheets based planar supercapacitors can potentially be a significant feature of the next-generation flexible energy storage devices such as supercapacitors, lithium batteries, and fuel cells, establishing a novel and important model to fabricate highly flexible power devices.

The planar supercapacitors based on 2D in-plane hybrid design have achieved impressive electrochemical performance compared with traditional 3D sandwich-type supercapacitors based on TMOs such as MnO_x, MoO_x, and VO_x.[34−36] (see SI part S11) They also exhibit the significant performance enhancement over graphene-only based supercapacitors in aqueous electrolytes with higher energy and power density, as shown in Figure 4F. For previously reported planar supercapacitors based on graphene-only thin films, the densely packed layer structure of graphene-only nanosheets will hinder efficient charge transport, especially for the electrolyte ion diffusion. To mitigate this problem, we established the novel 2D hybrid structures based on 2D hybrids of δ-MnO_2 nanosheets integrated on graphene sheets. The heterogeneous integration of δ-MnO_2 ultrathin nanosheets onto graphene can potentially relieve the densely stacking problem as that in the graphene-only thin films, and thus allow for more electrolyte ions to penetrate efficiently into the hybridized film and for effective utilization of more active surface areas. Moreover, the uniquely hybridized δ-MnO_2/graphene interlayer areas provide additional interfaces, where the conducting graphene could greatly facilitate electron conduction during the charging/discharging process. In our case, the material selection of hexagonal δ-MnO_2 nanosheets is also a key for enhancing the performance of planar supercapacitors, since δ-MnO_2 nanosheets bring more side-exposed manganese atoms, introducing extra surfaces and serving as the chemical active sites for the pseudocapacitive reactions during the charge/discharge process.

In summary, we have fabricated for the first time a novel, high-performance in-plane supercapacitor based on hybrid nanostructures of quasi-2D ultrathin MnO_2/graphene nanosheets. The hybrid 2D nanostructures based planar supercapacitors demonstrate the impressive electrochemical performance with a high specific capacitance of 267 F/g at current density of 0.2 A/g and excellent rate capability and cycling performance with capacitance retention of 92% after 7000 charge/discharge cycles. More importantly, given the high microscopic compressibility and macroscopic extensibility of the hybridized planar structure, the as-fabricated planar supercapacitors display extraordinary mechanical flexibility and stability under various bending states from being curved, folded to rolled, with >90% capacitance retention after folded thousands of times. These rationally designed planar supercapacitors represent a promising direction for building future-generation high-performance, flexible energy storage devices as the power back-ups for stretchable/flexible electronic devices.

■ ASSOCIATED CONTENT

Supporting Information

Detailed experimental synthesis procedures and supplementary characterizations including TEM, AFM, XPS, Tyndall effect, and EIS; a table used to evaluate specific capacitance of our planar supercapacitor with traditional sandwich-type supercapacitors. This material is available free of charge via the Internet at http://pubs.acs.org.

■ AUTHOR INFORMATION

Corresponding Author

*E-mail: czwu@ustc.edu.cn; yxie@ustc.edu.cn; ghyu@austin.utexas.edu.

Notes

The authors declare no competing financial interest.

■ ACKNOWLEDGMENTS

C.W. and Y.X. acknowledges the financial support by the National Basic Research Program of China (No. 2009CB939901), National Natural Science Foundation of China (No. 21222101, 11074229, 11132009, 11079004, J1030412), Program for New Century Excellent Talents in University, and the Fundamental Research Funds for the Central Universities (No. WK2340000035 and WK2310000024). G.Y. acknowledges the start-up funding support from Cockrell School of Engineering at the University of Texas at Austin.

■ REFERENCES

(1) Gates, B. D. *Science* **2009**, *323*, 1566−1567.
(2) Gao, W.; Singh, N.; Song, L.; Liu, Z.; Reddy, A. L. M.; Ci, L.; Vajtai, R.; Zhang, Q.; Wei, B.; Ajayan, P. M. *Nat. Nanotechnol.* **2011**, *6*, 496−500.
(3) Park, S.-I.; Xiong, Y.; Kim, R.-H.; Elvikis, P.; Meitl, M.; Kim, D.-H.; Wu, J.; Yoon, J.; Yu, C.-J.; Liu, Z.; Huang, Y.; Hwang, K.-c.; Ferreira, P.; Li, X.; Choquette, K.; Rogers, J. A. *Science* **2009**, *325*, 977−981.
(4) Bae, S.; Kim, H.; Lee, Y.; Xu, X.; Park, J.-S.; Zheng, Y.; Balakrishnan, J.; Lei, T.; Ri Kim, H.; Song, Y. I.; Kim, Y.-J.; Kim, K. S.; Ozyilmaz, B.; Ahn, J.-H.; Hong, B. H.; Iijima, S. *Nat. Nanotechnol.* **2010**, *5*, 574−578.
(5) Ju, S.; Li, J.; Liu, J.; Chen, P.-C.; Ha, Y.-g.; Ishikawa, F.; Chang, H.; Zhou, C.; Facchetti, A.; Janes, D. B.; Marks, T. J. *Nano Lett.* **2007**, *8*, 997−1004.
(6) Yamada, T.; Hayamizu, Y.; Yamamoto, Y.; Yomogida, Y.; Izadi-Najafabadi, A.; Futaba, D. N.; Hata, K. *Nat. Nanotechnol.* **2011**, *6*, 296−301.
(7) Wu, Z.; Chen, Z.; Du, X.; Logan, J. M.; Sippel, J.; Nikolou, M.; Kamaras, K.; Reynolds, J. R.; Tanner, D. B.; Hebard, A. F.; Rinzler, A. G. *Science* **2004**, *305*, 1273−1276.
(8) Yu, W. J.; Lee, S. Y.; Chae, S. H.; Perello, D.; Han, G. H.; Yun, M.; Lee, Y. H. *Nano Lett.* **2011**, *11*, 1344−1350.
(9) Pech, D.; Brunet, M.; Durou, H.; Huang, P.; Mochalin, V.; Gogotsi, Y.; Taberna, P.-L.; Simon, P. *Nat. Nanotechnol.* **2010**, *5*, 651−654.
(10) Chmiola, J.; Largeot, C.; Taberna, P.-L.; Simon, P.; Gogotsi, Y. *Science* **2010**, *328*, 480−483.
(11) Lin, J.; Zhang, C.; Yan, Z.; Zhu, Y.; Peng, Z.; Hauge, R. H.; Natelson, D.; Tour, J. M. *Nano Lett.* **2012**, *13*, 72−78.
(12) Conway, B. E. *J. Electrochem. Soc.* **1991**, *138*, 1539−1548.
(13) Naoi, K.; Simon, P. *Electrochem. Soc. Interface* **2008**, *17*, 34−37.
(14) Simon, P.; Gogotsi, Y. *Nat. Mater.* **2008**, *7*, 845−854.
(15) Lu, X.; Wang, G.; Zhai, T.; Yu, M.; Gan, J.; Tong, Y.; Li, Y. *Nano Lett.* **2012**, *12*, 1690−1696.
(16) Lang, X.; Hirata, A.; Fujita, T.; Chen, M. *Nat. Nanotechnol.* **2011**, *6*, 232−236.
(17) Yu, G.; Hu, L.; Vosgueritchian, M.; Wang, H.; Xie, X.; McDonough, J. R.; Cui, X.; Cui, Y.; Bao, Z. *Nano Lett.* **2011**, *11*, 2905−2911.
(18) Yoo, J. J.; Balakrishnan, K.; Huang, J.; Meunier, V.; Sumpter, B. G.; Srivastava, A.; Conway, M.; Mohana Reddy, A. L.; Yu, J.; Vajtai, R.; Ajayan, P. M. *Nano Lett.* **2011**, *11*, 1423−1427.

(19) Feng, J.; Sun, X.; Wu, C.; Peng, L.; Lin, C.; Hu, S.; Yang, J.; Xie, Y. *J. Am. Chem. Soc.* **2011**, *133*, 17832−17838.
(20) Yu, G.; Xie, X.; Pan, L.; Bao, Z.; Cui, Y. *Nano Energy* **2012**, DOI: 10.1016/j.nanoen.2012.10.006.
(21) Devaraj, S.; Munichandraiah, N. *J. Phys. Chem. C* **2008**, *112*, 4406−4417.
(22) Marcano, D. C.; Kosynkin, D. V.; Berlin, J. M.; Sinitskii, A.; Sun, Z.; Slesarev, A.; Alemany, L. B.; Lu, W.; Tour, J. M. *ACS Nano* **2010**, *4*, 4806−4814.
(23) Park, S.; An, J.; Potts, J. R.; Velamakanni, A.; Murali, S.; Ruoff, R. S. *Carbon* **2011**, *49*, 3019−3023.
(24) Omomo, Y.; Sasaki, T.; Wang, L.; Watanabe, M. *J. Am. Chem. Soc.* **2003**, *125*, 3568−3575.
(25) Coleman, J. N.; Lotya, M.; O'Neill, A.; Bergin, S. D.; et al. *Science* **2011**, *331*, 568−571.
(26) Xu, Y.; Bai, H.; Lu, G.; Li, C.; Shi, G. *J. Am. Chem. Soc.* **2008**, *130*, 5856−5857.
(27) Stoller, M. D.; Park, S.; Zhu, Y.; An, J.; Ruoff, R. S. *Nano Lett.* **2008**, *8*, 3498−3502.
(28) Zhi, M.; Xiang, C.; Li, J.; Li, M.; Wu, N. *Nanoscale* **2013**, *5*, 72−88.
(29) Liu, C.; Yu, Z.; Neff, D.; Zhamu, A.; Jang, B. Z. *Nano Lett.* **2010**, *10*, 4863−4868.
(30) Chen, C.; Fan, C.; Lee, M.; Chang, J. *J. Mater. Chem.* **2012**, *22*, 7697−7700.
(31) Yan, J.; Fan, Z.; Wei, T.; Qian, W.; Zhang, M.; Wei, F. *Carbon* **2010**, *48*, 3825−3833.
(32) Jurewicz, K.; Frackowiak, E.; Béguin, F. *Appl. Phys. A: Mater. Sci. Process.* **2004**, *78*, 981−987.
(33) Wang, G.; Lu, X.; Ling, Y.; Zhai, T.; Wang, H.; Tong, Y.; Li, Y. *ACS Nano* **2012**, *6*, 10296−10302.
(34) Wu, C.; Xie, Y. *Energy Environ. Sci.* **2010**, *3*, 1191−1206.
(35) Wu, Z.; Ren, W.; Wang, D.; Li, F.; Liu, B.; Cheng, H. *ACS Nano* **2010**, *4*, 5835−5842.
(36) Mai, L.; Yang, F.; Zhao, Y.; Xu, X.; Xu, L.; Luo, Y. *Nat. Commun.* **2011**, *2*, 381.

■ NOTE ADDED AFTER ASAP PUBLICATION

Figure 3 was inadvertently cropped in the version published ASAP on April 16, 2013. The corrected version was re-posted on April 17, 2013.